Production of O_2 on icy satellites by electronic excitation of low-temperature water ice

M. T. Sieger, W. C. Simpson & T. M. Orlando

W. R. Wiley Environmental Molecular Sciences Laboratory, Pacific Northwest National Laboratory, MS K8-88, PO Box 999, Richland, Washington 99352, USA

The signature of condensed molecular oxygen has been reported in recent optical-reflectance measurements of the jovian moon Ganymede[1], and a tenuous oxygen atmosphere has been observed on Europa[2]. The surfaces of these moons contain large amounts of water ice, and it is thought that O_2 is formed by the sputtering of ice by energetic particles from the jovian magnetosphere[3–8]. Understanding how O_2 might be formed from low-temperature ice is crucial for theoretical and experimental simulations of the surfaces and atmospheres of icy bodies in the Solar System. Here we report laboratory measurements of the threshold energy, cross-section and temperature dependence of O_2 production by electronic excitation of ice in vacuum, following electron-beam irradiation. Molecular oxygen is formed by direct excitation and dissociation of a stable precursor molecule, rather than (as has been previously thought) by diffusion and chemical recombination of precursor fragments. The large cross-section for O_2 production suggests that electronic excitation plays an important part in the formation of O_2 on Ganymede and Europa.

Lanzerotti *et al.*[9] were the first to use data from space-probe measurements of the jovian magnetosphere to examine energetic ion sputtering of the galilean satellites; their work was subsequently extended by Johnson *et al.*[10,11]. More recently, Ip *et al.*[8] used data from the Galileo spacecraft to assess ion sputtering of Ganymede. The reported heavy-ion and proton bombardment flux is between 10^8 and 10^{11} particles per cm^2 per s; the vacuum ultraviolet photon and electron flux ranges are expected to be similar. All of these studies concluded that the sputtering of water ice plays a central role in the evolution of the icy moons, their atmospheres, and the plasma composition of the jovian magnetosphere.

It is well known that the sputtering of low-temperature ice by fast, light ions is determined by the electronic excitations produced in the ice, rather than direct momentum transfer via collisions of the ions with water molecules[5,12]. This phenomenon, termed 'electronic sputtering', includes all loss of material from the ice as a result of electronic excitation by photons, electrons or fast ions. Fast-ion bombardment of ice is important on Ganymede and Europa, and most of the ion energy is deposited into direct excitations and secondary electron production[8–12]. Secondary electrons can then cause further excitations, forming an 'electronic cascade' by which a single incident ion produces thousands of electronic excitations. Excited water molecules may then break apart[13,14], ejecting molecular fragments from the surface or trapping them in the ice. To assess the role of electronic excitations in the production of molecular oxygen, we have studied low-energy (<100 eV) electron bombardment of thin ice films. Thin water-ice films are relevant to conditions present on icy outer Solar System bodies, because the surfaces of these bodies are ice-enriched. The production and redistribution of gas-phase water molecules by meteorite impacts, sputtering and thermal desorption would suggest that even exposed rocks are coated with thin layers of water ice or frost. The use of electron bombardment as an excitation source has many advantages over high-energy ions, because the low excitation density, absence of direct momentum-transfer processes, and negligible local heating allow us to examine the purely electronic processes involved in O_2 formation. Once the mechanism of O_2 formation in ice is understood, it can then be applied to a diverse range of excitation sources (for example, photons, electrons and ions) and to diverse environments, such as the jovian moons, comets, icy grains, and other outer Solar System bodies.

The experiments were performed in an ultra-high vacuum system ($\sim 10^{-10}$ torr) equipped with a pulsed low-energy electron gun and a quadrupole mass spectrometer. The 5–100 eV monoenergetic electron beam supplied a time-averaged electron flux of $\sim 6 \times 10^{13}$ electrons per cm^2 per s. Amorphous ice samples were prepared by vapour-depositing thin (~ 150 Å) films of D_2O on a clean Pt(111) substrate at 110 K, at a rate of 4–8 monolayers per min. D_2O was used instead of H_2O to help distinguish ejected D_2O from background gases. Other than an isotope shift in the temperature scale, it has been shown in sputtering experiments[15] that D_2O and H_2O ice behave similarly. The desorption products were detected with the quadrupole mass spectrometer in an 'electron beam on–beam off' mode which allowed for background subtraction. Other details of the apparatus and sample preparation have been published elsewhere[14].

Large amounts of O_2 (typically one molecule per 1,000 incident electrons) were generated from our ice samples during electron bombardment. The electron energy threshold was 10 ± 2 eV, corresponding to valence electronic excitation of ice, and the yield generally increased with ice temperature. Oxygen is not produced immediately on bombardment; an 'incubation dose' is required before the yield becomes appreciable. A similar incubation dose has been observed in ion- and vacuum ultraviolet photon-induced sputtering of ice[16,17], and implies a two-step (precursor-mediated) sputtering mechanism. To demonstrate that a precursor is needed to form O_2, and to investigate its lifetime, we exposed regions of a fresh ice sample, selected to write out "O_2" using the electron beam steering optics, to a $\sim 10^{15}$ cm^{-2} dose of 50 eV (significantly above threshold) electrons. The O_2 yield was then measured as the electron beam was rastered quickly over the entire sample, forming an image of the O_2-producing regions (Fig. 1). The contrast between the irradiated and non-irradiated regions shows that O_2 is produced via

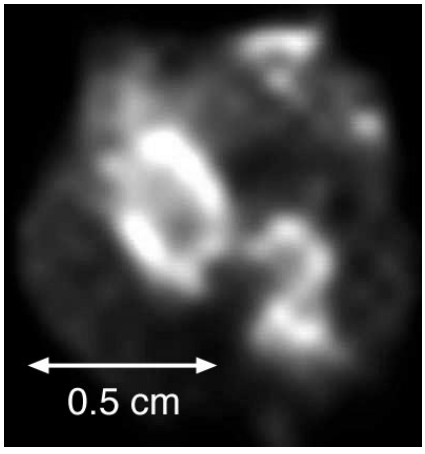

Figure 1 Image of the O_2 yield as a function of electron-beam spot position on an ice thin-film sample. Regions selected to spell out "O_2" were exposed to a $\sim 10^{15}$ cm^{-2} dose of 50-eV electrons, at a sample temperature of 120 K. The sample is 1 cm in diameter, and the electron beam has a spot size of ~ 0.4 mm^2. After the initial exposure, the electron beam was rastered over the sample, and the O_2 yield was measured as a function of the beam spot position. Bright and dark areas correspond to high and low O_2 yields, respectively. The circular profile of the sample is evident, as are the symbols marking the pre-bombarded areas. The contrast between the irradiated and non-irradiated regions demonstrates that O_2 is produced by a stable precursor. The elapsed time between 'writing' and 'reading' was ~ 1 h; the precursor species must therefore be stable on at least this timescale.

a precursor which is stable on the timescale of at least an hour at 120 K, suggestive of a stable molecular species, instead of a short-lived reactive species (such as atomic O).

By observing how the incubation dose depends on electron energy and ice temperature, we can extract detailed information about the O_2 formation mechanism. Measurements of the O_2 yield as a function of electron dose are shown in Fig. 2 for selected electron energies and ice temperatures. The yield is initially zero, rises with increasing dose, and eventually reaches a steady-state value. There are only a limited number of kinetic models which are consistent with our data. In all cases, the steady-state yield is limited by the precursor formation rate, whereas the dose needed to reach steady state is determined by the rate at which precursors form O_2.

The data in Fig. 2 show that the steady-state O_2 yield increases with both electron energy and ice temperature. The dose needed to reach steady state depends on electron energy (Fig. 2a), but is independent of temperature (Fig. 2b, c). The data from Fig. 2b have been normalized at their steady-state values and plotted together in Fig. 2c to show more clearly the independence of the incubation dose on temperature. From these observations we can draw two conclusions: the precursor formation mechanism depends on temperature, while the process by which precursors are converted to O_2 does not depend on temperature in the temperature range studied.

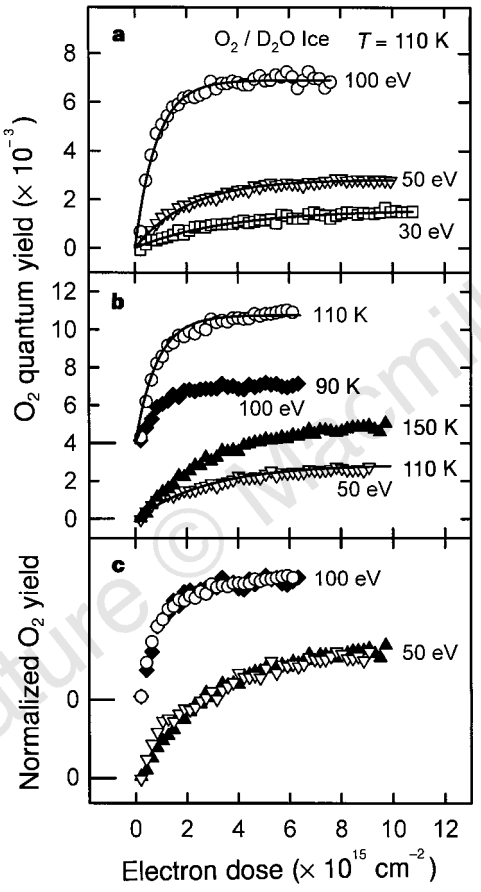

Figure 2 O_2 yield versus electron dose. **a**, O_2 quantum yield (molecules per incident electron) as a function of total electron dose for selected electron energies, at an ice temperature of 110 K. Open circles, 100 eV; open triangles, 50 eV; open squares, 30 eV. The O_2 yield increases with electron energy, and the dose needed to reach steady state decreases with increasing energy. **b**, O_2 quantum yield as function of total electron dose, for selected ice temperatures and electron energies (the 100 eV data has been offset by $+4 \times 10^{-3}$ for clarity). Filled diamonds, 100 eV at 90 K; filled triangles, 50 eV at 150 K; other symbols as in **a**. The yield increases with temperature, but the dose needed to reach steady state does not. **c**, The data from normalized at their steady-state values and plotted together, to show more clearly the independence of the rise to steady state on temperature. The 100-eV data are offset for clarity. All data were acquired at a fixed electron flux (6×10^{13} cm^{-2} s^{-1}) and measured as a function of time. Once the yield has saturated, it is linear in the instantaneous electron flux, and the energy threshold is 10 ± 2 eV (referenced to the vacuum level). Plotted with the data are best-fit curves generated with the precursor dissociation model (solid lines).

The increase in the sputter yield with dose and temperature has traditionally been interpreted as arising from the build-up and thermal diffusion of radical precursors which chemically react to form O_2. This hypothesis, however, cannot explain our results, as the process by which precursors form O_2 is temperature independent. The observed incubation-dose behaviour is also inconsistent with thermal diffusion in the precursor formation step, as diffusion models predict a quadratic rise in the yield near zero dose, while the data is clearly linear.

A two-step 'precursor dissociation' mechanism reproduces all the salient features of the data, and suggests to us a new interpretation of thermal effects in electronic sputtering of ice. A water molecule is first excited by an electron, photon or ion impact. Small changes in the structure or dynamic relaxation of ice can cause the excited state lifetime, and therefore the dissociation probability, to increase with temperature. We propose that the temperature dependence of O_2 production is in the lifetime of the electronic excited states leading to dissociation of water molecules. There is recent evidence that excited-state lifetimes in ice do increase with temperature[14,18], in a manner suggestive of changes in the local hydrogen bonding. The dissociation fragments (O, OH) then reactively scatter to form a stable precursor molecule, possibly HO_2 or H_2O_2, which are known to be produced in irradiated ice[6,19,20]. A second electronic excitation then directly dissociates the precursor molecule to form O_2.

Estimates of the precursor creation and dissociation cross-sections obtained by fitting the data to our model (Fig. 2, solid lines) are listed in Table 1, along with the measured cross-section for the stimulated desorption of D_2O. We estimate that the steady-state O_2 production rate at Ganymede from secondary electrons alone should exceed 10^7 cm^{-2} s^{-1}. The total (secondaries plus direct excitation) production rate is likely to be at least an order of magnitude higher. The measured threshold of ~10 eV is accessible to Lyman-α photons (10.2 eV), and so O_2 may also be produced by direct solar illumination. The measured cross-sections imply that the concentration of precursors in the near-surface region of ice is <1%, and so may elude all but the most sensitive spectroscopic detection[21]. However, O_2 may accumulate in the ice or become trapped at mineral/ice interfaces, giving rise to the observed absorption spectra[1,7]. Subsequent reactive interactions of water fragments with trapped O_2 can then form ozone (O_3), which has been observed on Ganymede[22,23].

The source of the temperature dependence implies that changes in the local electronic structure are more important than thermal diffusion for chemical processes in the electronic sputtering of ice. A prediction of our model is that the precursor concentration at steady state is a function only of temperature, and not electron/ion/photon flux, suggesting that the precursor concentration should be directly proportional to surface temperature; this is in agreement with recent observations showing that on Ganymede, more con-

Table 1 O_2 precursor creation and dissociation

	Cross-section (cm^2)		
Desorption product	$E_i = 100$ eV	$E_i = 50$ eV	$E_i = 30$ eV
D_2O	1×10^{-18}		
O_2 precursor creation	2×10^{-18}	8×10^{-19}	5×10^{-19}
O_2 precursor dissociation	3×10^{-16}	1×10^{-16}	8×10^{-17}

Shown are estimated cross-sections (to within an order of magnitude) for D_2O-stimulated desorption, and O_2 precursor formation and dissociation for selected electron energies E_i, at a sample temperature of 110 K. The O_2 precursor creation and precursor dissociation cross-sections are obtained from a fit of the precursor dissociation model to the data of Fig. 2. The total O_2 production cross-section at steady state is essentially the O_2 precursor creation cross-section, as the rate-limiting step in O_2 formation is the precursor formation rate.

densed O_2 is present at the equatorial latitudes than at the colder poles[4]. The mechanism proposed here is applicable to electronic excitations caused by essentially any radiation source (electrons, ions or photons), provides a quantitative understanding of O_2 formation in ice, and indicates that oxygen is probably also produced on other icy outer Solar System bodies. □

Received 8 December 1997; accepted 27 April 1998.

1. Spencer, J. R., Calvin, W. M. & Person, M. J. Charge-coupled device spectra of the Galilean satellites: Molecular oxygen on Ganymede. *J. Geophys. Res.* **100,** 19049–19056 (1995).
2. Hall, D. T., Strobel, D. F., Feldman, P. D., McGrath, M. A. & Weaver, H. A. Detection of an oxygen atmosphere on Jupiter's moon Europa. *Nature* **373,** 677–679 (1995).
3. Calvin, W. M., Johnson, R. E. & Spencer, J. R. O_2 on Ganymede: Spectral characteristics and plasma formation mechanisms. *Geophys. Res. Lett.* **23,** 673–676 (1996).
4. Calvin, W. M. & Spencer, J. R. Latitudinal distribution of O_2 on Ganymede: Observations with the Hubble Space Telescope. *Icarus* **130,** 505–516 (1997).
5. Johnson, R. E. Sputtering of ices in the outer solar system. *Rev. Mod. Phys.* **68,** 305–312 (1996).
6. Johnson, R. E. & Quickenden, T. I. Photolysis and radiolysis of water ice on outer solar system bodies. *J. Geophys. Res.* **102,** 10985–10996 (1997).
7. Vidal, R. A., Bahr, D., Baragiola, R. A. & Peters, M. Oxygen on Ganymede: Laboratory studies. *Science* **276,** 1839–1842 (1997).
8. Ip, W.-H., Williams, D. J., McEntire, R. W. & Mauk, B. Energetic ion sputtering effects at Ganymede. *Geophys. Res. Lett.* **24,** 2631–2634 (1997).
9. Lanzerotti, L. J., Brown, W. L., Poate, J. M. & Augustyniak, W. M. On the contribution of water products from Galiliean satellites to the Jovian magnetosphere. *Geophys. Res. Lett.* **5,** 155–158 (1978).
10. Johnson, R. E. *Energetic Charged-particle Interactions with Atmospheres and Surfaces* (Springer, Berlin, 1990).
11. Johnson, R. E., Lanzerotti, L. J., Brown, W. L. & Armstrong, T. P. Erosion of Galilean satellite surfaces by Jovian magnetosphere particles. *Science* **212,** 1027–1030 (1980).
12. Brown, W. L., Lanzerotti, L. J., Poate, J. M. & Augustyniak, W. M. "Sputtering" of ice by MeV light ions. *Phys. Rev. Lett.* **40,** 1027–1030 (1978).
13. Kimmel, G. A. & Orlando, T. M. Low-energy (5-120 eV) electron-stimulated dissociation of amorphous D_2O ice: $D(^2S)$, $O(^3P_{2,1,0})$ and $O(^1D_2)$ yields and velocity distributions. *Phys. Rev. Lett.* **75,** 2606–2609 (1995).
14. Sieger, M. T., Simpson, W. C. & Orlando, T. M. Electron-stimulated desorption of D^+ from D_2O ice: Surface structure and electronic excitations. *Phys. Rev. B* **56,** 4925–4937 (1997).
15. Brown *et al.* Erosion and molecule formation in condensed gas films by electronic energy loss of fast ions. *Nucl. Inst. Methods* **198,** 1–8 (1982).
16. Reimann, C. T. *et al.* Ion-induced molecular ejection from D_2O ice. *Surf. Sci.* **147,** 227–240 (1984).
17. Westley, M. S., Baragiola, R. A., Johnson, R. E. & Baratta, G. A. Photodesorption from low-temperature water ice in interstellar and circumsolar grains. *Nature* **373,** 405–407 (1995).
18. Simpson, W. C. *et al.* Dissociative electron attachment in nanoscale ice films: Temperature and morphology effects. *J. Chem. Phys.* **107,** 8668–8678 (1997).
19. Bednarek, J., Plonka, A., Hallbrucker, A., Mayer, E. & Symons, M. C. R. Hydroperoxyl radical generation by gamma-irradiation of glassy water at 77 K. *J. Am. Chem. Soc.* **118,** 9387–9390 (1996).
20. Taub, I. A. & Eiben, K. Transient solvated electron, hydroxyl, and hydroperoxy radicals in pulse-irradiated crystalline ice. *J. Chem. Phys.* **49,** 2499–2513 (1968).
21. Noll, K. S., Johnson, R. E., McGrath, M. A. & Caldwell, J. J. Detection of SO_2 on Callisto with the Hubble Space Telescope. *Geophys. Res. Lett.* **24,** 1139–1142 (1997).
22. Noll, K. S., Johnson, R. E., Lane, A. L., Domingue, D. L. & Weaver, H. A. Detection of ozone on Ganymede. *Science* **273,** 341–343 (1996).
23. Lacombe, S. *et al.* Electron-induced synthesis of ozone in a dioxygen matrix. *Phys. Rev. Lett.* **79,** 1146–1149 (1997).

Acknowledgements. We thank G. A. Kimmel for discussions. This work was supported by the US Department of Energy, Office of Basic Energy Sciences, Chemical Physics Program. Pacific Northwest National Laboratory is operated for the US Department of Energy by Battelle Memorial Institute.

Correspondence and requests for materials should be addressed to T.M.O. (e-mail: tm_orlando@pnl. gov).

Fluctuation-induced diffusive instabilities

David A. Kessler* & Herbert Levine†

* *Minerva Center and Department of Physics, Bar-Ilan University, Ramat Gan, Israel*

† *Department of Physics, University of California, San Diego, La Jolla, California 92093-0319, USA*

The formation of complex patterns in many non-equilibrium systems, ranging from solidifying alloys to multiphase flow[1], nonlinear chemical reactions[2] and the growth of bacterial colonies[3,4], involves the propagation of an interface that is unstable to diffusive motion. Most existing theoretical treatments of diffusive instabilities are based on mean-field approaches, such as the use of reaction–diffusion equations, that neglect the role of fluctuations. Here we show that finite fluctuations in particle number can be essential for such an instability to occur. We study, both analytically and with computer simulations, the planar interface separating different species in the simple two-component reaction A + B → 2A (which can also serve as a simple model of bacterial growth in the presence of a nutrient). The interface displays markedly different dynamics within the reaction–diffusion treatment from that when fluctuations are taken into account. Our findings suggest that fluctuations can provide a new and general pattern-forming mechanism in non-equilibrium growth.

We consider a slightly modified version[5] of an "infection" model due to Blumen *et al.*[6,7]. There are two types of particles, infectious (A) and non-infected but susceptible (B). Both particle types move diffusively on a lattice, with no constraint on multiple occupancy, with differing rates D_A and D_B. A B particle which is co-located with an A particle has some probability per unit time of becoming infected, that is, changing to an A. At the mean-field level in which we ignore particle number fluctuations, the dynamics of this system is describable via the coupled reaction–diffusion equations:

$$\frac{\partial c_A}{\partial t} = \nabla^2 c_A + c_A c_B$$
$$\frac{\partial c_B}{\partial t} = D\nabla^2 c_B - c_A c_B \qquad (1)$$

Here we have scaled out the reaction rate and furthermore scaled space so as to eliminate D_A in the first equation; D is defined as the ratio D_B/D_A. Formally, this equation can be obtained as the limit of the underlying Markov process when the average number of particles per site, N, goes to infinity. In the special case $D = 1$, this system reduces to the Fisher equation[8].

Our interest here is in interface propagation, namely the process whereby introduction of some number of A particles at the left edge of a finite region filled with B particles at some initial concentration c_B^0 leads to the development of a moving front. The velocity of such a front in the reaction–diffusion approximation follows from the marginal stability principle[9–11]:

$$v_{MS} = 2\sqrt{c_B^0} \qquad (2)$$

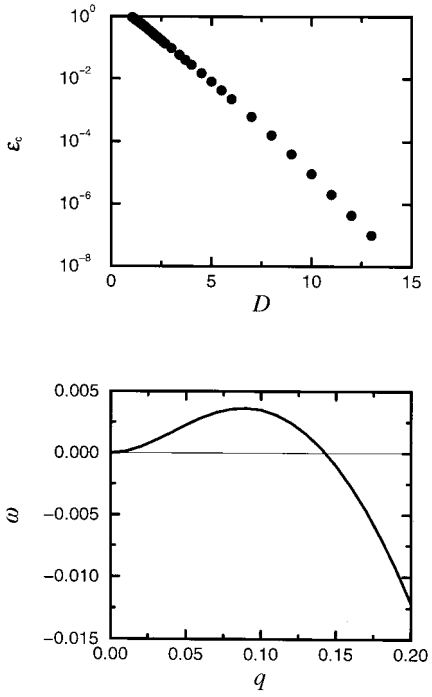

Figure 1 Results of stability analysis. Top, dependence of the critical value ϵ_c of the cut-off as a function of the diffusion-constant ratio D. Bottom, spectrum at $D = 10$, $\epsilon = 0.0014$. See Methods for details.